Analytical derivation of the geometric factor of a particle detector having circular or rectangular geometry

Analytical derivation of the geometric factor of a particle detector having circular or rectangular geometry

G R Thomas and D M Willis
SRC, Radio and Space Research Station, Ditton Park, Slough, SL3 9JX

MS *received 12 October 1971, in revised form 18 November 1971*

Abstract The geometric factor of a particle detector having either circular or rectangular geometry is derived analytically. Both isotropic and '$\cos^2\theta$' variations of intensity are considered. An approach based on 'shadow areas' is applied to the case of particles passing through two unequal circular areas, and it is proved that the results are identical with those obtained previously using an approach based on the direct integration of 'infinitesimal areas'. This latter approach is then used for the case of two unequal rectangular areas, which has not been considered previously. The analytical results confirm those obtained previously using numerical techniques.

1 Introduction

Geometric factor calculations have an important application in the data analysis of a wide variety of experiments involving particle detectors. Thus, the intensity I of an incident particle distribution is related to the detector counting rate N by the equation $I=N/G$, where G is the geometric factor. In this paper we consider the geometric factor defined by two infinitely thin, plane, coaxial, parallel areas with known separation. The incident particles are assumed to have rectilinear trajectories passing through both areas. Analytical results are presented for areas which are either circular or rectangular.

Two approaches have been used in previous studies of geometric factors. The first approach involves a calculation of the shadow area projected by one area on the other as a function of the angle of incidence θ of the incoming radiation with respect to the detector axis. A single integration with respect to θ then yields the geometric factor. The shadow area approach is used in §2 for the case of unequal circular areas. In the second approach the two areas are each divided into infinitesimal elements, resulting in a quadruple integral for the geometric factor. This integral is evaluated in §3 for the case of unequal rectangular areas.

2 Circular geometry

The relevant geometry is illustrated in figure 1, in which R_1 and R_2 are the radii of the two (unequal) areas, and Z is their separation. We assume $R_2>R_1$, but the final result is independent of this assumption. Consider that component of the

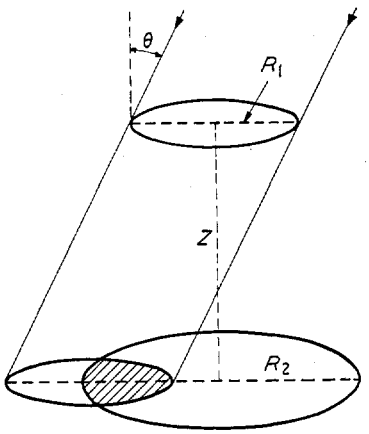

Figure 1 Relevant geometry for the application of the 'shadow area' approach to unequal circular areas

radiation which is incident at an angle θ to the detector axis. The effective area presented to this radiation is the projection of the shadow area (cross-hatched in figure 1) in the plane normal to the incident radiation. For angles of incidence between 0 and θ_L, where the limiting angle of incidence θ_L is defined by

$$\theta_L=\arctan\{(R_2-R_1)/Z\} \quad (R_2>R_1) \tag{1}$$

the whole of the upper (smaller) area will be projected on to the lower (larger) area. The shadow area is then simply πR_1^2. Consider now angles of incidence between θ_L and θ_M, where

$$\theta_M=\arctan\{(R_1+R_2)/Z\} \tag{2}$$

is the maximum angle of incidence for which linear trajectories pass through both upper and lower areas. In this case the shadow area S is given by

$$\begin{aligned}S=&R_1^2\arccos\left(\frac{R_1^2-R_2^2+Z^2\tan^2\theta}{2R_1Z\tan\theta}\right)\\&-R_1^2\left(\frac{R_1^2-R_2^2+Z^2\tan^2\theta}{2R_1Z\tan\theta}\right)\\&\times\left\{1-\left(\frac{R_1^2-R_2^2+Z^2\tan^2\theta}{2R_1Z\tan\theta}\right)^2\right\}^{1/2}\\&+R_2^2\arccos\left(\frac{R_2^2-R_1^2+Z^2\tan^2\theta}{2R_2Z\tan\theta}\right)\\&-R_2^2\left(\frac{R_2^2-R_1^2+Z^2\tan^2\theta}{2R_2Z\tan\theta}\right)\\&\times\left\{1-\left(\frac{R_2^2-R_1^2+Z^2\tan^2\theta}{2R_2Z\tan\theta}\right)^2\right\}^{1/2}.\end{aligned} \tag{3}$$

For an isotropic distribution of incident particles the contribution to the geometric factor at angle θ is the product of the projected shadow area and the solid angle $2\pi\sin\theta\delta\theta$. The total geometric factor is therefore given by

$$G=2\pi^2R_1^2\int_0^{\theta_L}\sin\theta\cos\theta\,d\theta+2\pi\int_{\theta_L}^{\theta_M}S\sin\theta\cos\theta\,d\theta \tag{4}$$

where S is given by (3). These integrals can be evaluated using standard mathematical techniques to give

$$G=\tfrac{1}{2}\pi^2[R_1^2+R_2^2+Z^2-\{(R_1^2+R_2^2+Z^2)^2-4R_1^2R_2^2\}^{1/2}] \tag{5}$$

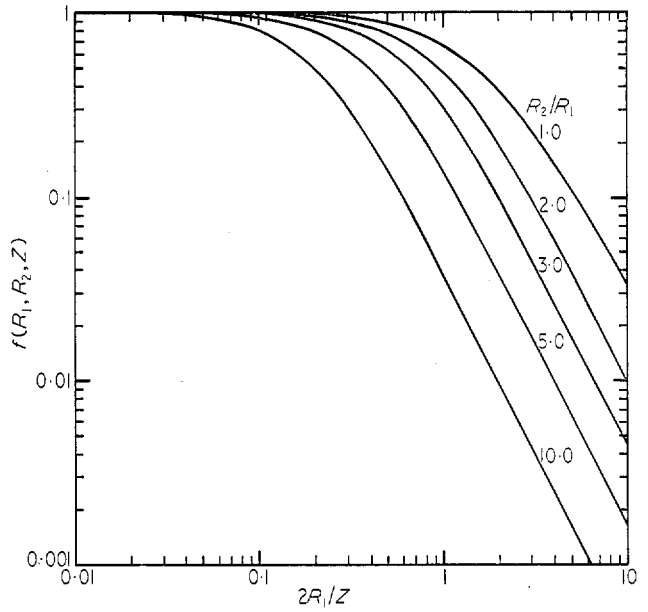

Figure 2 Correction factor f calculated for unequal circular areas as a function of $2R_1/Z$ for various values of R_2/R_1

which is symmetric in R_1, R_2. This result, derived using the shadow area approach, agrees with that obtained by Heristchi (1967): cf. his equation (2), using the infinitesimal areas approach. The same result was also obtained by Manno *et al.* (1970): cf. their equation (14), again using the infinitesimal areas approach. The latter authors suggested that this result would also be obtained using the shadow area approach, but they did not perform the final integration with respect to θ. We have proved rigorously that the two approaches yield identical results.

In the limiting case R_1^2, $R_2^2 \ll Z^2$ equation (5) reduces to the form

$$G \simeq \frac{\pi^2 R_1^2 R_2^2}{Z^2}. \tag{6}$$

Thus the geometric factor is approximated by the product of the areas divided by the square of their separation. This is a useful result which is often used to approximate the geometric factor when the separation of the areas is large compared with their radii. The accuracy of the approximation may be expressed in terms of a correction factor f defined by

$$f = \frac{G(R_1, R_2, Z)}{\pi^2 R_1^2 R_2^2 / Z^2}. \tag{7}$$

In figure 2 the factor f is plotted as a function of the ratio $(2R_1/Z)$ for various values of the ratio $R_2/R_1 \geqslant 1$. Values of f for $R_1 > R_2$ are not plotted in the figure as they would not provide any additional information, owing to the symmetry of f with respect to R_1 and R_2.

Gillespie (1970) approximated the integration over infinitesimal areas by the summation of a difference equation. From his table II, for equal circular areas, we have normalized the geometric factor calculated for $\Delta R/R = 0{\cdot}05$ to the ratio A^2/H^2 (his notation). The resulting values of the factor f are in agreement with our analytically derived values to within 0·1 %.

Corresponding results can be derived for a '$\cos^2\theta$' variation of intensity. These results are applicable to measurements of cosmic rays at sea level (Sandström 1965). The analysis proceeds exactly as above, except that an additional $\cos^2\theta$ term appears in equation (4), i.e.

$$G = 2\pi^2 R_1^2 \int_0^{\theta_L} \sin\theta \cos^3\theta \, d\theta + 2\pi \int_{\theta_L}^{\theta_M} S \sin\theta \cos^3\theta \, d\theta \tag{8}$$

where S is again given by (3). These integrals may also be evaluated using standard mathematical techniques to yield the result

$$G = \frac{\pi^2}{4}\left[R_1^2 + R_2^2 - \frac{\{Z^2(R_1^2+R_2^2)+(R_2^2-R_1^2)^2\}}{\{(R_1^2+R_2^2+Z^2)^2 - 4R_1^2R_2^2\}^{1/2}}\right]. \tag{9}$$

The same result was obtained by Heristchi (1967) using the infinitesimal areas approach, which again demonstrates the equivalence of the two approaches. Brunberg (1958) derived the particular result for equal circular areas using the shadow area approach. In the limiting case R_1^2, $R_2^2 \ll Z^2$ equation (9) reduces to equation (6), as for the isotropic case.

3 Rectangular geometry

Figure 3 illustrates the relevant geometry, the two rectangular areas having sides of length $2X_1$, $2Y_1$ and $2X_2$, $2Y_2$, with Z being their separation. In the figure $X_2 > X_1$ and $Y_2 > Y_1$,

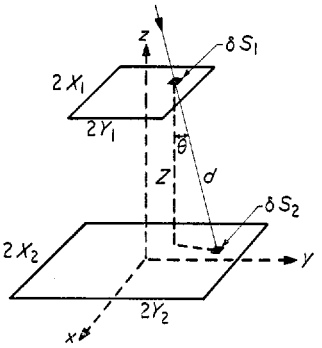

Figure 3 Relevant geometry for the application of the 'infinitesimal areas' approach to unequal rectangular areas

but the final result is independent of this assumption. Consider that component of the radiation which is incident at an angle θ to the detector axis and passes through the two small elements of area $\delta S_1 = \delta x_1 \delta y_1$ and $\delta S_2 = \delta x_2 \delta y_2$. These areas are situated at (x_1, y_1, Z) and $(x_2, y_2, 0)$, respectively. For an isotropic intensity the geometric factor presented to this radiation is

$$\delta G = \delta S_1 \cos\theta \times \delta S_2 \cos\theta / d^2 \tag{10}$$

where d is the distance between the infinitesimal areas. Substituting for δS_1 and δS_2, and using the relationships $d^2 = Z^2 + (x_2 - x_1)^2 + (y_2 - y_1)^2$ and $\cos\theta = Z/d$, equation (10) may be expressed as follows:

$$\delta G = \frac{Z^2 \, \delta x_1 \, \delta y_1 \, \delta x_2 \, \delta y_2}{\{Z^2 + (x_2 - x_1)^2 + (y_2 - y_1)^2\}^2}. \tag{11}$$

The total geometric factor is then given by

$$G = Z^2 \int_{-X_1}^{X_1} \int_{-Y_1}^{Y_1} \int_{-X_2}^{X_2} \int_{-Y_2}^{Y_2} \frac{dx_1 \, dy_1 \, dx_2 \, dy_2}{\{Z^2 + (x_2 - x_1)^2 + (y_2 - y_1)^2\}^2}. \tag{12}$$

This multiple integral can be evaluated to give

$$
\begin{aligned}
G=&\,2\{Z^2+(X_1+X_2)^2\}^{1/2}\\
&\times\left[(Y_1+Y_2)\arctan\frac{(Y_1+Y_2)}{\{Z^2+(X_1+X_2)^2\}^{1/2}}\right.\\
&\qquad\left.-(Y_2-Y_1)\arctan\frac{(Y_2-Y_1)}{\{Z^2+(X_1+X_2)^2\}^{1/2}}\right]\\
&-2\{Z^2+(X_2-X_1)^2\}^{1/2}\\
&\times\left[(Y_1+Y_2)\arctan\frac{(Y_1+Y_2)}{\{Z^2+(X_2-X_1)^2\}^{1/2}}\right.\\
&\qquad\left.-(Y_2-Y_1)\arctan\frac{(Y_2-Y_1)}{\{Z^2+(X_2-X_1)^2\}^{1/2}}\right]\\
&+2\{Z^2+(Y_1+Y_2)^2\}^{1/2}\\
&\times\left[(X_1+X_2)\arctan\frac{(X_1+X_2)}{\{Z^2+(Y_1+Y_2)^2\}^{1/2}}\right.\\
&\qquad\left.-(X_2-X_1)\arctan\frac{(X_2-X_1)}{\{Z^2+(Y_1+Y_2)^2\}^{1/2}}\right]\\
&-2\{Z^2+(Y_2-Y_1)^2\}^{1/2}\\
&\times\left[(X_1+X_2)\arctan\frac{(X_1+X_2)}{\{Z^2+(Y_2-Y_1)^2\}^{1/2}}\right.\\
&\qquad\left.-(X_2-X_1)\arctan\frac{(X_2-X_1)}{\{Z^2+(Y_2-Y_1)^2\}^{1/2}}\right]\\
&+Z^2\ln\frac{\{Z^2+(X_1+X_2)^2+(Y_2-Y_1)^2\}\times\{Z^2+(X_2-X_1)^2+(Y_1+Y_2)^2\}}{\{Z^2+(X_1+X_2)^2+(Y_1+Y_2)^2\}\times\{Z^2+(X_2-X_1)^2+(Y_2-Y_1)^2\}}
\end{aligned}
\tag{13}
$$

which is symmetric in X_1, X_2 and Y_1, Y_2, and is also unchanged by interchanging X and Y.

In the limiting case X_1^2, Y_1^2, X_2^2, $Y_2^2 \ll Z^2$ this reduces to

$$G \simeq \frac{16X_1Y_1X_2Y_2}{Z^2} \tag{14}$$

i.e. the geometric factor is again approximated by the product of the areas divided by the square of their separation. The special case of equal rectangular areas was considered by Witmer and Pomerantz (1948). Their equation (45) corresponds to (13) with $X_1=X_2=X$ and $Y_1=Y_2=Y$. The accuracy of the approximation (14) in this special case is then specified by the correction factor

$$f=\frac{G(X,Y,Z)}{16X^2Y^2/Z^2}. \tag{15}$$

This factor is plotted in figure 4 as a function of the ratio $2X/Z$ for various values of the ratio Y/X. The symmetry of the results with respect to X and Y may be verified by comparing the curves for $Y/X=0{\cdot}5$ and $0{\cdot}1$ with those for $2{\cdot}0$ and $10{\cdot}0$.

Values of f can also be derived from table I of Gillespie (1970), which refers to numerical summation for equal square areas. His values of the geometric factor for $\Delta S/S=0{\cdot}05$ have been normalized using the ratio A^2/H^2 (his notation) and the resulting values are within $0{\cdot}25\%$ of our analytically derived values for $Y/X=1$. Similarly, values of f can be derived from the calculations of Stern (1960), also for equal square areas. His values agree with our analytical values to within $0{\cdot}4\%$.

The modification for a $\cos^2\theta$ variation of intensity involves an additional $\cos^2\theta$ term in equation (10) so that $\delta G=$

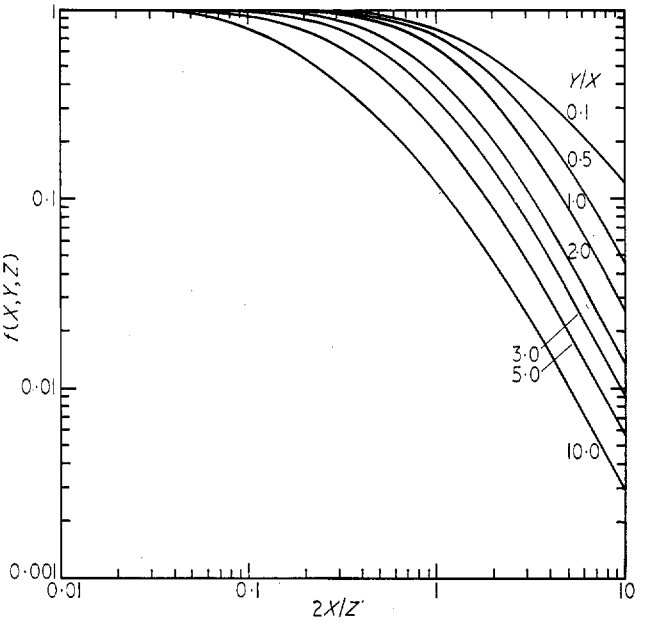

Figure 4 Correction factor f calculated for equal rectangular areas as a function of $2X/Z$ for various values of Y/X

$\delta S_1\delta S_2\cos^4\theta/d^2$. Equation (12) for the geometric factor then becomes

$$G=Z^4\int_{-X_1}^{X_1}\int_{-Y_1}^{Y_1}\int_{-X_2}^{X_2}\int_{-Y_2}^{Y_2}\frac{dx_1\,dy_1\,dx_2\,dy_2}{\{Z^2+(x_2-x_1)^2+(y_2-y_1)^2\}^3} \tag{16}$$

and the final result is

$$
\begin{aligned}
G=&\frac{\{Z^2+2(X_1+X_2)^2\}}{2\{Z^2+(X_1+X_2)^2\}^{1/2}}\\
&\times\left[(Y_1+Y_2)\arctan\frac{(Y_1+Y_2)}{\{Z^2+(X_1+X_2)^2\}^{1/2}}\right.\\
&\qquad\left.-(Y_2-Y_1)\arctan\frac{(Y_2-Y_1)}{\{Z^2+(X_1+X_2)^2\}^{1/2}}\right]\\
&-\frac{\{Z^2+2(X_2-X_1)^2\}}{2\{Z^2+(X_2-X_1)^2\}^{1/2}}\\
&\times\left[(Y_1+Y_2)\arctan\frac{(Y_1+Y_2)}{\{Z^2+(X_2-X_1)^2\}^{1/2}}\right.\\
&\qquad\left.-(Y_2-Y_1)\arctan\frac{(Y_2-Y_1)}{\{Z^2+(X_2-X_1)^2\}^{1/2}}\right]\\
&+\frac{\{Z^2+2(Y_1+Y_2)^2\}}{2\{Z^2+(Y_1+Y_2)^2\}^{1/2}}\\
&\times\left[(X_1+X_2)\arctan\frac{(X_1+X_2)}{\{Z^2+(Y_1+Y_2)^2\}^{1/2}}\right.\\
&\qquad\left.-(X_2-X_1)\arctan\frac{(X_2-X_1)}{\{Z^2+(Y_1+Y_2)^2\}^{1/2}}\right]\\
&-\frac{\{Z^2+2(Y_2-Y_1)^2\}}{2\{Z^2+(Y_2-Y_1)^2\}^{1/2}}\\
&\times\left[(X_1+X_2)\arctan\frac{(X_1+X_2)}{\{Z^2+(Y_2-Y_1)^2\}^{1/2}}\right.\\
&\qquad\left.-(X_2-X_1)\arctan\frac{(X_2-X_1)}{\{Z^2+(Y_2-Y_1)^2\}^{1/2}}\right]
\end{aligned}
\tag{17}
$$

Geometric factor of a particular detector

In the limiting case X_1^2, Y_1^2, X_2^2, $Y_2^2 \ll Z^2$ equation (17) reduces to equation (14), as for the isotropic case. For the special case of equal rectangular areas, equation (50) of Witmer and Pomerantz (1948) corresponds to (17) with $X_1 = X_2 = X$ and $Y_1 = Y_2 = Y$. As in the isotropic case, a correction factor f may then be defined to specify the accuracy of the approximation (14). In the case of two equal square areas, Tidman and Ogilvie (1957) have evaluated f for a $\cos^2\theta$ variation of intensity, as a function of the angle β between the detector axis and the vertical. For the four values of the ratio $2X/Z$ considered by Tidman and Ogilvie, 0·05, 0·1, 0·5, 0·75, the analytical values of f for $Y/X = 1$ are 1·00, 0·99, 0·80, 0·65. The computed values given in figure 2 of Tidman and Ogilvie for $\beta = 0$ appear to be in good agreement with these, except for $2X/Z = 0{\cdot}05$ when their numerical value seems to be greater than unity. Values of f for equal square areas can also be derived from the calculations of Stern (1960). They are within 0·3% of our analytical values.

4 Conclusions

Geometric factors have been derived analytically for particle detectors having either circular or rectangular geometry, and for both isotropic and $\cos^2\theta$ variations of intensity. In the case of circular geometry we have proved rigorously that the shadow area approach yields analytical results identical with those obtained by previous workers using the infinitesimal areas approach. For rectangular geometry, we have extended previous work using the infinitesimal areas approach to include the case of unequal areas.

Acknowledgments

We are indebted to Mr K B Ahlstedt, a vacation worker from the Royal University of Technology, Stockholm, for verifying the integrations in §3. The work described in this paper was carried out at the Radio and Space Research Station and is published with the permission of the Director.

Note added in proof

Since submitting this paper for publication, it has been brought to our attention that the results for an isotropic intensity (equations (5) and (13)) have been derived independently by Sullivan (1971).

References

Brunberg E-Å 1958 *Ark. Fys.* **14** 195–254

Gillespie C R 1970 *Rev. sci. Instrum.* **41** 42–3

Heristchi D J 1967 *Nucl. Instrum. Meth.* **47** 39–44

Manno V, Page D E and Shaw M L 1970 *ELDO/ESRO Scient. Tech. Rev.* **2** 363–79

Sandström A E 1965 *Cosmic Ray Physics* (Amsterdam: North Holland)

Stern D 1960 *Nuovo Cim.* Suppl. **16** 153–8

Sullivan J D 1971 *Nucl. Instrum. Meth.* **95** 5–11

Tidman D A and Ogilvie K W 1957 *Nuovo Cim.* **6** 735–8

Witmer E E and Pomerantz M A 1948 *J. Franklin Inst.* **246** 293–309

Journal of Physics E: Scientific Instruments 1972 Volume 5
Printed in Great Britain

An absolute detector for metastable rare gas atoms

F B Dunning
Department of Physics, University College, Gower Street, London WC1E 6BT

MS *received 6 September 1971*

Abstract An absolute metastable atom detector which utilizes the principle of secondary electron emission from a metal surface is described. The secondary electron emission coefficient of the detection surface is maintained constant by continuous deposition of metal on to the surface. The detector is suitable for the continuous measurement of a metastable atom beam flux of the order of 3×10^6 atoms/s or greater in a background gas pressure as high as 1 μTorr.

1 Introduction

Several methods have been used in the past to detect the presence of metastable atoms and molecules. The techniques most commonly used fall into two basic categories – those that rely on optical absorption or electric fields to raise the metastable level to one that decays radiatively and those that utilize the internal energy of the metastable atom to eject an electron from either a surface or another free atom or molecule.

Surface detection is a versatile and convenient technique in experiments where beams of metastable atoms are used. In this type of detector metastable atoms impinge on a metallic surface at which they give up their internal energy to an electron in the surface material, which may then be ejected. The current of electrons leaving the surface provides a measure of the incident metastable atom flux. A necessary condition is that the work function of the surface be less than the internal energy of the incident metastable atom. Fluxes of a number of different metastable atoms have been measured using this technique (for instance, Schulz and Fox 1957, Sholette and Muschlitz 1962, Fite and Brackmann 1963, Tang *et al.* 1971), but previous detectors have employed either undefined surfaces or well-defined surfaces that could only be maintained for a few minutes.

The aim of the present work was to develop and calibrate absolutely a detection system, using a well defined atomically clean surface, that could be used for continuous absolute measurements of a metastable atom beam flux even under the practical conditions of background gas pressures as high as 1 μTorr, which are often encountered in crossed beam collision experiments.

The use of a contaminated undefined surface as an absolute detector must always be suspect since the value of the